Available online at www.sciencedirect.com

ScienceDirect

Energy Procedia 92 (2016) 949 – 955

Energy Procedia

6th International Conference on Silicon Photovoltaics, SiliconPV 2016

DopLa solar cells with texturized front surface

Isidro Martín*, Arnau Coll, Gema López, Pablo R. Ortega, Juan M. López-González, Ramon Alcubilla

Departament d'Enginyeria Electrònica, Universitat Politècnica de Catalunya, C/Jordi Girona 1-3, Mòdul C4, 08034 Barcelona, Spain

Abstract

In this work, we report on improving efficiency of DopLa cells fabricated on p-type substrates. This type of solar cells has all the highly-doped regions based on laser doping from dielectric films resulting in a very simple fabrication process. Depending on the dopant type, emitter regions or high/low doping junctions related to base contacts can be created. The emitter regions are located at the rear surface in order to be contacted by a continuous metal film without penalizing in shadowing losses, while the front surface shows a typical finger grid configuration with the base contacts under the metal. In a previous work, the reported efficiency was limited by optical losses at the front planar surface. As a consequence, we focus on the introduction of a texturized front surface to the device. Firstly, we characterize the contact formation by laser processing on texturized surfaces by SEM image showing that the size of the contacted region is difficult to determine. By measuring contact resistance and surface recombination velocity, we deduce that the laser process of such surfaces leads to a contacted region which is smaller than the one where passivation is lost. The obtained information is included in 3D simulations to get the optimum size of the contacts, i.e. optimum laser power. Additionally, a new front grid metallization is introduced in order to reduce shadowing. Due to the rear emitter configuration of these devices, front surface recombination is crucial for collecting photogenerated carriers. Thus, optimum laser power is very close to the minimum to obtain a reliable contact. Finally, 2x2 cm^2 solar cells are fabricated with a best efficiency of 17.0 %.

Peer review by the scientific conference committee of SiliconPV 2016 under responsibility of PSE AG.

Keywords: DopLa cell; laser doping; back-junction; c-Si solar cells.

* Corresponding author. Tel.: +34-93-4054193; fax: +34-93-4016756.
E-mail address: isidro.martin@upc.edu

Peer review by the scientific conference committee of SiliconPV 2016 under responsibility of PSE AG.
doi:10.1016/j.egypro.2016.07.106

1. Introduction

In the recent years, laser doping processes have attracted the attention of the crystalline silicon (c-Si) photovoltaic community due to its potential cost-saving applications. Laser processing of dielectric films to create highly-doped regions have been investigated by different groups [1-3]. Our research activities in this field have been focused on the development of a novel structure of crystalline silicon (c-Si) solar cell called DopLa (Doped by Laser) cell where all the highly-doped regions are created by laser doping from dielectric films. In particular, the n^+ regions are formed by processing a phosphorus-doped silicon carbide film stack ($SiC_x(n)$)[4], while the p^+ regions are based on aluminum oxide/silicon carbide (Al_2O_3/SiC_x) film [5]. Apart from working as dopant sources, these films provide c-Si surface passivation and anti-reflection properties. In this way, the fabrication procedure of DopLa cells can be simplified to cleaning, film deposition, laser doping and metallization. The resulting DopLa structure for double-side contacted p-type solar cells can be seen in figure 1,(a) and another example of this approach can be found in ref. [6], where the laser processed regions are applied onto Interdigitated Back-Contacted solar cells.

A conversion efficiency of 12.6 % was previously reported in reference [7] for DopLa cells with similar structure than the one represented in figure 1,(a). The main limitations for those cells were the optical losses, since front surface was not texturized, and ohmic losses due to the long distance between base contacts located at the front surface (1 mm). Keeping the same solar cell structure, in this work we report on the impact of two strategies introduced to overcome these limitations: a texturized front surface to minimize optical losses and a redesign of the front contact distribution.

2. Experimental

For solar cell fabrication, we used 280 μm-thick 2.5 Ωcm FZ c-Si 4” wafers cut into quarters as substrates that were textured at the front surface. As a first step, Al_2O_3 films were deposited by Atomic Layer Deposition technique with a thickness of 50 nm using Tri-Methyl Aluminum (TMA) and water as gas precursors. In order to activate the c-Si surface passivation properties of these films, we annealed them at 400 ºC for 10 minutes. Next, we deposited a 30 nm-thick dielectric SiC_x film by PECVD on the front surface as a capping layer. This film shows a refractive index of 2.0 at λ = 632 nm indicating a close to stoichiometric composition and it is transparent to photons with wavelengths beyond 500 nm. This film combination results in a suitable front anti-reflection layer and in an improved aluminum doping efficiency after laser processing, as demonstrated in ref. [8]. In addition, the SiC_x film prevents the front Al_2O_3 to be etched in the subsequent complete RCA cleaning needed to prepare the surface for the $SiC_x(n)$ stack deposition on the rear surface. The $SiC_x(n)$ stack consists of a thin (~ 4 nm) intrinsic silicon-rich amorphous silicon carbide film followed by a ~15nm-thick phosphorus-doped amorphous silicon layer. Finally, a 80 nm dielectric silicon carbide identical to the one capping the Al_2O_3 layer at the front surface is deposited on top of both films in order to isolate them from the metal contacts, except for the laser processed regions, and improve light trapping properties of the device.

The n^+ emitter was defined at the rear surface following an hexagonal matrix using a Q-switched Nd:YAG laser (StarMark SMP 100II Rofin-Baasel) emitting at 1064 nm in TEM00. The distance between neighbor laser spots or *pitch* is 250 μm, since previous results demonstrated that closer distances lead to worse results [9]. The power used for the n^+ region formation was 0.95 W. After laser processing, we metallized the emitters by Ti/Pd/Ag stack deposited by e-beam through a shadowing mask. The laser processed at the front surface consists of laser spots separated 250 μm along the finger direction followed by a 3 μm-thick aluminum thermal evaporation. The metal grid was defined by a lithography step and chemical etching of the aluminum between fingers leading to 2x2 cm^2 solar cells. The finished devices were characterize by 1 sun-illumination *J-V* measurements using Keithley SMU 2601B under standard conditions (25ºC, 100 mW/cm^2, AM1.5 g). The solar simulator used for these measurements is Oriel 94021A. External Quantum Efficiency measurements were carried out with QEX10 setup from PVMeasurements Inc. Device reflectance was measured with UV-VIS-NIR spectrometer Shimadzu 3600.

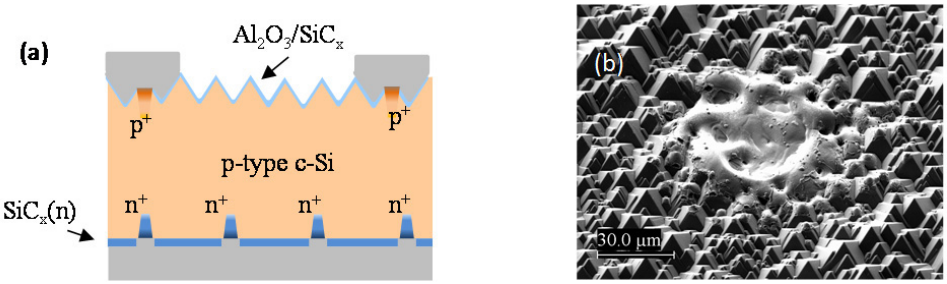

Fig. 1. (a) DopLa cell structure with the texturized front surface; (b) SEM image of a laser spot of 1.17 W on texturized surface.

3. Results and discussion

3.1. Determination of the contacted and high-recombination regions

In figure 1,(b), we show a SEM image of a contact made on texturized surface covered with Al_2O_3/ SiC_x stack at a laser power of 1.17 W. As it can be seen, pyramids are lost in the centre of the laser processed region due to the melting of the silicon and recrystallization process. The pyramids in the spot surroundings also show their peaks affected by the laser process and the dielectric layer is also removed. As a consequence, the definition of the contacted area once the metal is deposited onto it is difficult to determine. Additionally, surface recombination at the contact is expected to be much worse than for the flat surface case. The uneven surface results in a more stressful process probably leading to both non-uniform doping and low quality recrystallization. Moreover, the depassivated area affected by the laser is also difficult to define.

Based on the obtained SEM pictures, we focused our efforts on the measurement of both the contacted area and the high-recombination area. Firstly, we determined the contacted area by measuring the contact resistance of the laser spots and approximate them as circles with radius r_{cont}. In particular, we defined square arrays of laser spots and contact them with Aluminum while an ohmic contact was created on the other side of the test sample. The spots are separated 1 mm and can be considered as equal parallel resistors. Then, from the array measurement, the resistance associated with just one spot (r_{spot}) can be determined by dividing the total array resistance by the number of spots. The resistance of every point has two components: one related to the spreading resistance and the other one related to the specific contact resistance ρ_{cef}, as it can be seen in the following equation [10]:

$$r_{spot} = \frac{\rho_b r_{cont}}{2} \tan^{-1}\left(\frac{2w}{r_{cont}}\right) + \rho_{cef} \quad (1)$$

where ρ_b is the wafer resistivity (2.5 Ωcm) and w is the wafer thickness (280 µm). In equation (1), there are two unknown magnitudes: the contact radius (r_{cont}) and the specific contact resistance (ρ_{cef}). It is well known that Aluminum forms an ohmic contact on p-type c-Si with ρ_{cef} increasing when doping density is decreased. In our sample, the worst case is when the aluminum is directly contacting the base with no extra doping coming from the Al_2O_3/SiC_x stack. Following data reported in ref.[11] we can consider a maximum contact resistance of $5{\cdot}10^{-4}$ Ωcm^2 for a substrate doping density of $5.7{\cdot}10^{15}$ cm^{-3}. With such a contact resistance, we can deduce a contact radius applying equation (1). The results for laser powers ranging from 0.88 to 1.17 W are shown in figure 2,(a) with r_{cont} ranging from 22 to 35 µm. It must be mentioned that the assumption of negligible ρ_{cef} results in only 2-3 µm smaller r_{cont} values. As expected, contact radius increases with laser power indicating that a bigger area is contacted. The size of the contacted areas is comparable to the visually melted regions, as it can be seen for 1.17 W at figure 1,(b). Laser powers lower than 0.88 W do not create reliable contacts on the c-Si surface.

On the other hand, recombination at the contacts can be determined by measuring the lifetime degradation when laser processed area increases. The increase in the effective surface recombination velocity S_{eff} can be modelled using the following equation [12]:

$$S_{eff} = \frac{D}{w} \times \left[\frac{p}{2w\sqrt{\pi f_c}} \times \tan^{-1}\left(\frac{2w}{r_{rec}}\right) - e^{\left(-w/p\right)} + \frac{D}{f_c w S_{cont}} \right]^{-1} + \frac{S_{pas}}{1-f_c} \quad (2)$$

where p is the distance between contacts or *pitch*, D is the diffusion constant for minority carriers (D= 30.59 cm^2/s), S_{pas} is the surface recombination velocity at the passivated surfaces (S_{pas}= 9 cm/s, experimentally determined) and f_c is the laser processed area fraction assuming round spots with a radius of r_{rec} (f_c= $\pi r_{rec}^2/p^2$). Again we find two unknown magnitudes: the radius of the high recombination area (r_{rec}) and its surface recombination (S_{cont}). The results of test samples for 0.92 and 1.17 W are plotted in the inset of figure 2,(a) with the best fit using equation (2). Excellent agreement can be found for both samples when S_{cont}= 5·10^6 cm/s is used indicating that a non-passivated contact is created. Additionally, the corresponding radius of such highly recombining region is also included in figure 2,(a). From these two points an interpolation for the other laser powers can be done obtaining an estimation of the high-recombination region radius for every laser power. As it can be seen, the depassivated region has a higher radius than the electrical contact. Moreover, the r_{rec} value for 1.17 W is 55 µm which is much higher than the one suggested by the SEM picture shown in figure 1,(b) indicating that the laser process negatively impact on the passivation of laser spot surroundings. This conclusion agrees with a microscale characterization of these regions reported in reference [13] where it is demonstrated that surface passivation is degraded at the spot surroundings even for flat surfaces.

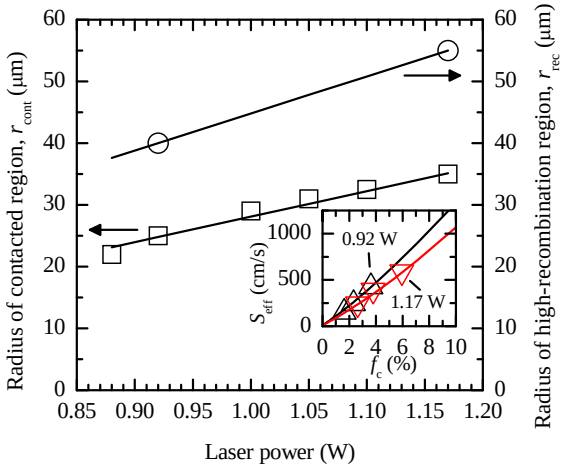

Fig. 2. Radius of the contacted region and radius of the high-recombination region as a dependence of laser power; (inset) dependence of S_{eff} on laser processed area fraction for laser powers of 0.92 and 1.17 W. Theoretical curves lead to r_{rec} of 55 and 43 µm for 1.17 and 0.92 W respectively.

3.2. 3D simulations

With all these data, we performed 3D simulations with Silvaco ATLAS to evaluate the maximum achievable efficiency of DopLa cells with a laser processed texturized front surface. Simulations are based on similar DopLa cell modeling reported in reference [7]. In particular, we used the same rear surface modeling, since the rear surface configuration has not been changed. Its main characteristics are Gaussian-profile phosphorus diffusions with a peak density of 10^{19} cm^{-3} and a junction depth of 1 µm modeling n$^+$ regions; a fundamental surface recombination velocity at the surface between n$^+$ regions of 3000 cm/s with a fixed charge density Q_f= 4.3·10^{11} cm^{-3} that creates an induced emitter; only intrinsic recombination processes are considered for bulk recombination. For the front texturized surface, we used the obtained r_{rec} and r_{cont} values for every laser power. The front reflectance of the texturized surface with the Al_2O_3/ SiC_x stack was measured on a test wafer and introduced into the simulations. In

addition, we introduce a new front contact configuration. In order to reduce ohmic losses, we shorten the distance between base contacts along the finger direction from 1 mm to 250 µm. On the other hand, the 90 µm-wide fingers are now separated 1.25 mm and the bus bar is defined as a frame in the cell perimeter and out of the cell area. With this configuration, the shadowing losses are reduced to 7.2 % compared to the 13.11 % with the previous front metal grid. A picture of a final device with this new metallization design can be seen in figure 4,(a). The calculated series resistance introduced by this metal grid is 0.24 Ωcm^2 which is also introduced in the simulations by means of a lumped resistor element.

As it can be seen in figure 3,(a) where simulation results are shown, fill factor (*FF*) slightly increases with higher laser powers due to a bigger contacted area at the front surface. On the contrary, open-circuit voltage (V_{oc}) decreases from 637 to 631 mV in the simulated range, because front surface recombination velocity is higher. It must be mentioned that V_{oc} values are mainly limited by recombination at the rear surface between laser processed regions, as it was deduced in reference [7]. However, the main impact of the front surface recombination increase occurs on the short-circuit current density (J_{sc}). The solar cell structure has a rear emitter configuration and, thus, recombination at the front surface plays a crucial role for carrier collection. The strong decrease in J_{sc} obtained with higher laser powers is translated to the efficiency (η) leading to the lowest laser powers as the best choice. For 0.88 and 0.92 W, the small increase in *FF* compensates the decrease in J_{sc} keeping efficiency almost constant for both values. Then, for the fabrication of the solar cells we used 0.92 W, since we have experimentally verified that some of the contacts at 0.88 W may fail due to laser power fluctuations. Finally, from simulations we concluded that the expected surface recombination velocity at the front surface (S_f) with this laser power and contact configuration is 28 cm/s.

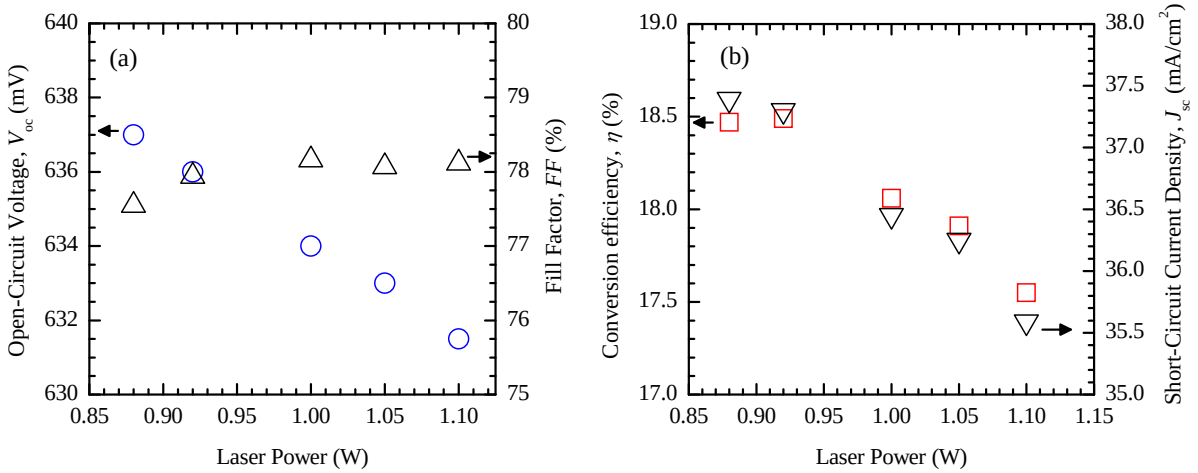

Fig. 3. (a) Open-circuit voltage and fill factor; (b) short-circuit current density and conversion efficiency determined from 3D simulations.

3.3. Results of fabricated solar cells

We fabricated solar cells as indicated in the experimental section with a laser power of 0.92 W for the front contact formation. The results of the best 2x2 cm^2 cell are shown in Table 1.

Table1. Photovoltaic figures of best 2x2 cm^2 DopLa cell.

J_{sc} (mA/cm^2)	V_{oc} (mV)	*FF* (%)	η (%)
36.5	624	74.6	17.0

As it can be seen, solar cell efficiency has been boosted up to 17.0 % from the previous 12.6 % reported in ref. [7]. The main reason for such a big increase is the improvement of J_{sc} due to the front surface configuration with reduced optical and electrical losses. In order to determine the front surface recombination velocity, we measure the External Quantum Efficiency (*EQE*) and the front reflection (R_f) of the solar cell. Then, the Internal Quantum Efficiency (*IQE*) can be calculated applying $IQE = EQE/(1-R_f)$. The level of the plateau of *IQE* in the visible range is strongly dependent of S_f. This parameter can be obtained by fitting the experimental *IQE* data with simple simulations with PC-1D of a rear emitter structure where we use the experimental value of R_f and the real thickness of the solar cell. An identical approach was used in ref. [9] demonstrating that more complex 3D simulations are not needed to get reliable S_f values. The obtained values of *EQE*, R_f and *IQE* are shown in figure 4,(b) together with the best fit based on PC-1D simulations that yields a S_f of 55 cm/s. Although this value is approximately a factor of two higher than expected from the one deduced from simulations, it is still a quite remarkable low value that results in only a J_{sc} loss of 0.8 mA/cm^2 respect to the simulated values. In addition, the difference in the IQE response for $\lambda <$ 450 nm is attributed to light absorption in the front SiC_x capping layer [14], which are not included in the simulations.

On the other hand, V_{oc} and *FF* values are also lower than expected. Taking into account the deduced S_f value and using again simple PC-1D simulations, we conclude that V_{oc} is limited by the recombination in the emitter. Moreover, solar cells with different rear pitch were fabricated leading to almost identical V_{oc} values of 622±2 mV. Consequently, the main recombination mechanism should be related to the surface between laser processed regions. On this surface, the value of Q_f is critical to determine the surface recombination properties and the ohmic losses related to the inversion layer induced by this charge. In fact, a slightly lower Q_f value than the one introduced in the simulations ($4.3 \cdot 10^{11}$ cm^{-2}) could explain both the lower V_{oc} and *FF*. This lower Q_f would increase rear surface recombination independently on laser processed area and would weaken the inversion channel that connects the n^+ regions increasing the ohmic losses and reducing FF. Although the mentioned problems in the rear surface, the introduction of a texturized front surface and the new front contact configuration demonstrates that DopLa cells could be a feasible solution for low-cost c-Si solar cells.

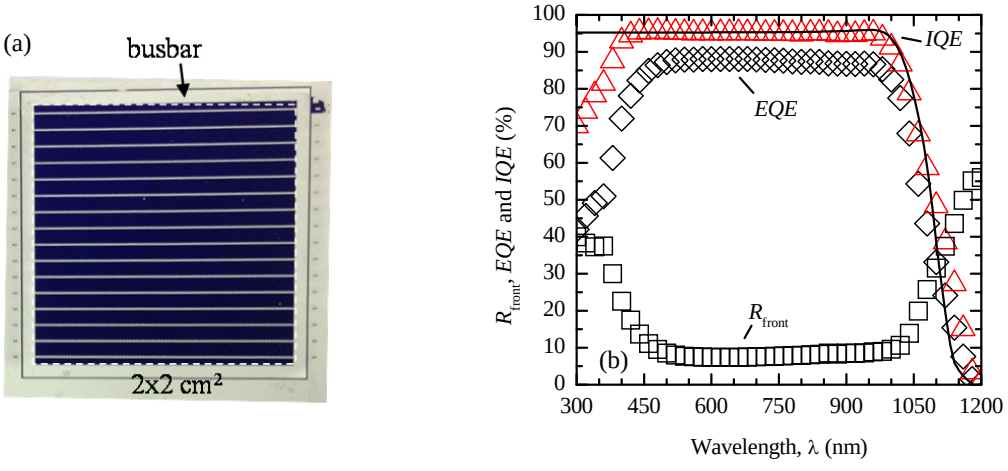

Fig. 4. (a) Picture of a finished DopLa solar cell where the busbar is defined at the cell perimeter out of the 2x2 cm^2 area; (b) EQE, IQE and R (symbols) of the best fabricated solar cell together with the PC-1D fit (line).

4. Conclusions

In this work, we have reported on the improvement in cell efficiency of DopLa cells fabricated on p-type substrates. In order to reduce optical losses, the impact of a front texturized surface has been characterized. The laser process leads to non-passivated contacts whose contacted area is lower than the high-recombination region. These results are attributed to the uneven surface leading to a detrimental effect on the doping distribution and

recrystallization quality. In addition, a new front metal grid is presented in order to minimize shadowing and ohmic losses. All these features were introduced to 3D simulations to calculate the maximum achievable efficiency and determine the optimum laser power to be applied in the solar cells. Due to the rear emitter configuration, the front surface passivation plays a crucial role in carrier collection and the optimum laser power is 0.92 W, very close to the lowest limit to create reliable contacts. Finally, solar cells were fabricated with a maximum efficiency of 17.0 %. The improvement in cell efficiency is mainly related to the new front surface features that allow low optical and electrical losses with S_f = 55 cm/s.

Acknowledgements

This work has been supported by the Spanish Government under project TEC 2014-59736-R and ENE2013-48629-C4-1-R and by the European Union's Seventh Framework Programme for research, technological development and demonstration under project HERCULES (Grant agreement: 608498).

References

[1] Steinhauser B, Kamp, M, Brand AA, Jäger U, Bartsch J, Benick J, Hermle M. "High-Efficiency n-Type Silicon Solar Cells: Advances in PassDop Technology and NiCu Plating on Boron Emitter", IEEE Journal of Photovoltaics 2016; 6: 419-425.

[2] B. Paviet-Salomon B, Gall S, Monna R, Manuela S, Slaouib A." Experimental and analytical study of saturation current density of laser-doped phosphorus emitters for silicon solar cells", Solar Energy Materials and Solar Cells 2011; 95: 2536-2539.

[3] Werner F, Larionova Y, Zielke D, Ohrdes T, Schmidt J. Aluminum-oxide-based inversion layer solar cells on n-type crystalline silicon: Fundamental properties and efficiency potential. Journal of Applied Physics 115, 073702 (2014).

[4] Martín I, Colina M, Orpella A, Voz C, De Vecchi S, Desrues T, Abolmasov S, Roca i Cabarrocas P, Alcubilla R, "Low recombination n+ regions created by n+ c-Si epitaxial layers and laser processing of phosphorus-doped SiC_x films", in: Proceedings of 27th European Photovoltaic Solar Energy Conference, Frankfurt, Germany, 2012, pp. 1519-1523.

[5] Ortega P, Martín I, Lopez G, Colina M, Orpella A, Voz C, Alcubilla R. "p-type c-Si solar cells based on rear side laser processing of Al_2O_3/SiC_x stacks", Solar Energy Materials and Solar Cells 2012; 106: 80-83.

[6] López G, Ortega P, Martín I, Voz C, Orpella A, Alcubilla R. "A new fabrication concept of "cold" IBC c-Si solar cell", submitted to Energy Procedia.

[7] I. Martín I, López-González JM, Colina M, Orpella A, Alcubilla R, "DopLacell: a new c-Si solar cell based on laser processing of dielectric films", in: Proceedings of 28th European Photovoltaic Solar Energy Conference, Paris, France, 2013, pp. 1519-1523.

[8] Martín I, Ortega P, Colina M, Orpella A, López G, Alcubilla R. Laser processing of Al_2O_3/a-SiC_x:H stacks: a feasible solution for the rear surface of high-efficiency p-type c-Si solar cells. Progress in Photovoltaics: Research and Applications 2013; 21: 1171-1175.

[9] Martín I, Coll A, López G, Ortega P, Desrues T, Orpella A, Alcubilla R. "TCO-free low-temperature p+ emitters for back-junction c-Si solar cells", Energy Procedia 2015; 77: 296 – 303.

[10] Denhoff MW. "An accurate calculation of spreading resistance", Journal of Physics D: Applied Physics 2006; 39: 1761–1765.

[11] G.P. Carver GP, Kopanski JJ, Novotny DB, Forman RA. "Specific Contact Resistivity of Metal-Semiconductor Contacts-A New, Accurate Method Linked to Spreading Resistance", IEEE Transactions on Electron Devices 1988; 35: 489-497.

[12] Plagwitz H, Brendel R."Analytical model for the diode saturation current of point-contacted solar cells", Progress in Photovoltaics,: Research and Applications 2006; 14: 1-12.

[13] Roigé A, Ossó JO, Martín I, Voz C, Ortega P, López-González JM, Alcubilla R, Vega LF. "Microscale Characterization of Surface Recombination at the Vicinity of Laser-Processed Regions in c-Si Solar Cells", IEEE Journal of Photovoltaics 2016; 6: 426-431.

[14] López G, Ortega P, Voz C, Martín I, Colina M, Morales AB, Orpella A, Alcubilla R. Surface passivation and optical characterization of Al_2O_3/a-SiC_x stacks on c-Si substrates. Beilstein Journal of Nanotechnology 2013; 4: 726.